NATIONAL ADVISORY COMMITTEE FOR AERONAUTICS

WARTIME REPORT

ORIGINALLY ISSUED
January 1940 as
Advance Confidential Report

BOUNDARY-LAYER TRANSITION ON THE N.A.C.A. 0012 AND 23012 AIRFOILS IN THE 8-FOOT HIGH-SPEED WIND TUNNEL

By John V. Becker

Langley Memorial Aeronautical Laboratory
Langley Field, Va.

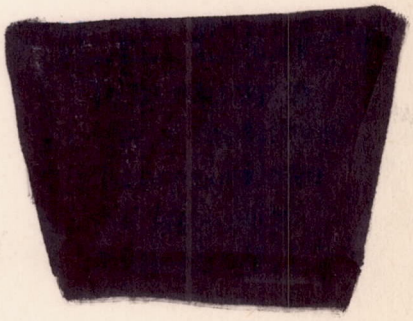

NACA

WASHINGTON

BOUNDARY-LAYER TRANSITION ON THE N.A.C.A. 0012 AND 23012 AIRFOILS IN THE 8-FOOT HIGH-SPEED WIND TUNNEL

By John V. Becker

SUMMARY

Determinations of boundary-layer transition on the N.A.C.A. 0012 and 23012 airfoils were made in the 8-foot high-speed wind tunnel over a range of Reynolds Numbers from 1,600,000 to 16,800,000. The results are of particular significance as compared with flight tests and tests in wind tunnels of relatively high turbulence because of the low turbulence in the high-speed tunnel.

A comparison of the results obtained on N.A.C.A. 0012 airfoils of 2-foot and 5-foot chord at the same Reynolds Number permitted an evaluation of the effect of compressibility on transition. The local skin friction along the surface of the N.A.C.A. 0012 airfoil was measured at a Reynolds Number of 10,000,000.

For all the lift coefficients at which tests were made, transition occurred in the region of estimated laminar separation at the low Reynolds Numbers and approached the point of minimum static pressure as a forward limit at the high Reynolds Numbers. The effect of compressibility on transition was slight. None of the usual parameters describing the local conditions in the boundary layer near the transition point served as an index for locating the transition point. As a consequence of the lower turbulence in the 8-foot high-speed tunnel, the transition points occurred consistently farther back along the chord than those measured in the N.A.C.A. full-scale tunnel.

INTRODUCTION

The study of transition from laminar to turbulent flow in the boundary layer of airfoils has recently been

stimulated by the discovery that extensive laminar layers exist in flight over the forward portion of very smooth wings (reference 1). The drag of an airfoil depends on the location of the point of transition from the low-drag laminar type of flow to the high-drag turbulent condition; and the prediction of drag from model tests therefore requires that the transition point, both in the wind tunnel and in flight, be known.

Most boundary-layer studies in the past have been restricted to flat plates or to simple shapes such as spheres and cylinders. (See references 2, 3, and 4.) The results have been of value as applied to airfoils chiefly in indicating the powerful effects on transition of wind-tunnel turbulence, surface roughness, and Reynolds Number. On airfoils operating through a wide range of angles of attack, the corresponding large change in static-pressure distribution is also important in controlling the extent of the laminar layer. For all airfoils, two general changes in static-pressure distribution on the upper surface take place as the angle of attack is increased: The point of minimum static pressure moves forward and the adverse pressure gradient behind this point becomes more severe. Recent tests in the N.A.C.A. full-scale wind tunnel (reference 5) showed that these factors cause the transition point to move forward with increasing angle of attack.

Investigations of boundary-layer transition in the N.A.C.A. 8-foot high-speed wind tunnel are significant because of the relatively low turbulence of the air stream. Sphere tests (reference 6) in this wind tunnel have shown approximately the same critical Reynolds number as in free air. However, more sensitive measurements made with hot-wire apparatus have indicated that the turbulence level of the 8-foot high-speed wind tunnel, while low, is still somewhat higher than in free air. The main purposes of the present investigation were: to locate points of transition in this wind tunnel on conventional, widely used airfoil sections as a basis of comparison with results obtained in streams of other turbulence; to obtain the effect of compressibility on boundary-layer transition; and to determine the skin-friction distribution at a high Reynolds Number as a basis for the prediction of airfoil drag.

In order to permit comparison with the tests made in the N.A.C.A. full-scale tunnel, which has a turbulence factor of 1.1 (reference 7), and with future flight tests, the N.A.C.A. 0012 airfoil was used in the greater portion of the present investigation. Less extensive tests of the N.A.C.A. 23012 airfoil were also made. By the use of N.A.C.A. 0012 airfoils of 2-foot and 5-foot chord, a

Reynolds Number range of 1,600,000 to 16,800,000 was attainable and, by a comparison of the results obtained on the two airfoils at the same Reynolds Number, the effect of compressibility could be evaluated.

Because the prediction of airfoil drag demands a knowledge of the skin friction for the laminar and the turbulent types of flow as well as of the location of the transition point, complete determinations were made of boundary-layer velocity profiles at a Reynolds Number of 10,250,000 to allow computation of the local skin-friction coefficients. These coefficients are compared with the approximations obtained by a suitable modification of theoretical flat-plate skin-friction coefficients.

Force measurements showing the drag increment due to controlled forward movement of the transition point were also made and the results are correlated with those of the skin-friction determinations.

This investigation was conducted during 1938.

APPARATUS AND METHODS

The N.A.C.A. 8-foot high-speed wind tunnel in which the investigation was conducted is a single-return, closed-throat, circular-section tunnel. The air speed is continuously controllable from approximately 75 to more than 500 miles per hour.

The airfoils employed in the tests spanned the test section of the tunnel (fig. 1). Two 5-foot-chord airfoils of N.A.C.A. 0012 and 23012 section were constructed of a wooden framework covered with 1/8-inch aluminum plate except for a short section at the leading edge, which was covered with steel and left unpainted to prevent erosion at high speeds. The aluminum-covered portion of the airfoils was spray-painted and finished with fine-grade water sandpaper until it was aerodynamically smooth. Close examination of the surface revealed barely perceptible surface waves at the lines of attachment of the metal sheet to the wooden formers, which could not be eliminated with this type of construction. So that the effect of these minute irregularities could be evaluated, another 5-foot-chord N.A.C.A. 0012 airfoil was built of solid wood; the surface of this airfoil could then be made aerodynamically fair as well as aerodynamically smooth.

A 2-foot-chord N.A.C.A. 0012 airfoil was built of solid duralumin. The surface of this airfoil was ideally smooth and fair so that test results for it could be directly compared with those for the solid-wood 5-foot-chord N.A.C.A. 0012 airfoil.

In the tests of the N.A.C.A. 0012 airfoils, velocities were determined at four heights above the airfoil surface chosen to permit a study of the velocity distribution in the boundary layer. Four small total-pressure tubes were mounted together with a single static tube in an arrangement similar to that described in reference 1.

The tubes used on the 5-foot-chord airfoils (fig. 2) were of stainless steel, 0.040-inch outside diameter, with a 0.003-inch wall thickness. The ends of the total-pressure tubes were flattened to an outside dimension of 0.012 inch for a length of one-half inch from the opening. The tubes were 2 inches long and were soldered into 1/16-inch copper tubes, which extended back along the surface of the airfoil to rubber tubing that was led along the trailing edge to manometers. A hemispherical plug was inserted into the end of the static tube and four 0.005-inch holes, equally spaced around the circumference, were drilled in the plane of the ends of the total-pressure tubes. The five tubes were soldered together on top of two 1/8-inch-high bridges to facilitate handling, adjustment of height, and attachment to the airfoil.

A similar set of survey tubes (fig. 3), approximately two-fifths the size of those used on the 5-foot-chord airfoil, was used for the tests on the 2-foot-chord airfoil.

The method of installing the tubes on the N.A.C.A. 0012 airfoils is shown in figure 1. Measurements were made with the bank of survey tubes located at 5-percent-chord intervals between 5 and 80 percent of the chord. The entire installation was attached to the airfoil by gummed cellulose tape covered with a thin coat of dope to prevent raising at the edges. In all the tests, the lowest tube was firmly sprung against the airfoil surface. The heights of the other tubes were set approximately to the desired values by means of thickness gages and then measured to the nearest 0.001 inch with a micrometer microscope.

The complete boundary-layer measurements required for the skin-friction determination of the 5-foot-chord N.A.C.A. 0012 airfoil were made by placing two banks of survey tubes

at the same chord station and adjusting the eight total-pressure tubes to include the full depth of the boundary layer.

Owing to the fact that the tubes were operating in a vertical velocity gradient, the indicated dynamic pressure was slightly higher than the true dynamic pressure at the geometric center of the tubes. The effective height, corresponding to the indicated dynamic pressure, was obtained from the results of reference 8, which show that about 20 percent of the over-all height of the tube should be added to the geometric height.

A simplified method of detecting transition was employed in the tests of the N.A.C.A. 23012 airfoil. Only the total pressure near the surface was measured by means of single total-pressure tubes of the same dimensions as those in the 4-tube survey heads used on the 5-foot N.A.C.A. 0012 airfoil (fig. 2). Only one tube being required at each station, it was possible to install tubes at all 14 stations at the same time. Care was taken to space the tubes a sufficient distance apart along the span so that the wake of one tube did not pass over the adjoining tubes. The theoretical static-pressure distribution was used to compute approximately the velocities corresponding to the total-pressure readings.

The effect of small surface irregularities in precipitating transition is well known. In the measurement of the drag increment associated with controlled movement of the transition point on the 5-foot-chord N.A.C.A. 0012 airfoil, transition was fixed at the desired chord station by a linen string doped across the span on both surfaces. Two sizes of string, 0.035 inch and 0.017 inch (outside dimensions after doping), were found to be equally effective in fixing the transition point. The same result was obtained by spraying a 1/2-inch strip of 0.0037-inch carborundum grains across the span, transition being assumed to start at the center of the strip.

TESTS

Determinations of boundary-layer transition on the N.A.C.A. 0012 airfoils were made at air speeds ranging from the minimum attainable, approximately 75 miles per hour, to 445 miles per hour. The section lift coefficients at

which the airfoils were tested were -0.57, -0.16, 0, 0.16, 0.33, and 0.65. Owing to structural limitations of the 5-foot-chord airfoil, the maximum allowable lift coefficient decreased as the air speed increased. Thus, at 445 miles per hour, only the zero-lift condition could be tested. There were no restrictions on the allowable lift coefficient of the 2-foot-chord airfoil in the speed range covered in these tests. Most of the tests of the N.A.C.A. 0012 airfoils were made with the metal-covered 5-foot-chord airfoil and the all-metal 2-foot-chord airfoil. The tests of the solid-wood 5-foot-chord airfoil were made after the main program had been completed and included only transition determinations at comparatively few test conditions.

The boundary-layer transition tests of the N.A.C.A. 23012 airfoil were made over a range of speeds of 80 to 445 miles per hour. The section lift coefficients, subject to the same restrictions as for the 5-foot-chord N.A.C.A. 0012 airfoils, were 0, 0.15, 0.30, and 0.65.

The boundary-layer momentum-loss determinations used in computing the local skin friction on the 5-foot-chord N.A.C.A. 0012 airfoil were made at zero lift at an air speed of 230 miles per hour.

The drag of the metal-covered 5-foot-chord N.A.C.A. 0012 airfoil was measured for each of the following conditions at speeds varying from 75 to 275 miles per hour: With the 0.035-inch string on upper and lower surfaces at the 2-, 5-, 10-, 15-, 20-, and 25-percent chord stations; with the 0.0037-inch carborundum grains at the same stations; and with the 0.017-inch string on upper and lower surfaces at the 10-percent chord station.

SYMBOLS

The symbols used in this report are defined as follows:

V, air speed (corrected for tunnel-wall constriction effect).

U, local velocity just outside boundary layer.

u, local velocity in boundary layer.

c, **airfoil chord.**

x, distance measured from leading edge along chord line.

y, distance measured normal to surface.

s, distance measured from forward stagnation point along surface. The relation between s and x for the N.A.C.A. 0012 airfoil is shown in table I.

δ, boundary-layer thickness.

δ^*, displacement boundary-layer thickness $\left[\int_0^{\delta}\left(1-\frac{u}{U}\right)dy\right]$

ν, kinematic viscosity.

μ, coefficient of viscosity.

R, Reynolds Number (Vc/ν).

R_s, local Reynolds Number (Us/ν).

R_δ, local Reynolds Number based on boundary-layer thickness $(U\delta/\nu)$.

R_{δ^*}, local Reynolds Number based on displacement boundary-layer thickness $(U\delta^*/\nu)$.

c_l, section lift coefficient.

c_{d_o}, section profile-drag coefficient.

c_{d_f}, section skin-friction drag coefficient.

c_f, local skin-friction coefficient.

P, coefficient of static pressure $\left(\frac{p_{local} - p_{stream}}{q}\right)$.

q, dynamic pressure $(1/2\ \rho V^2)$.

ρ, mass density of air.

M, momentum loss per unit span between boundary-layer flow and a corresponding mass flow imme-

diately outside boundary layer

$$\left[\int_0^{\delta} \rho u(U - u)\, dy\right].$$

N, thickness number $(1/3\ R_{\delta}*)$.

λ, Pohlhausen's boundary-layer profile-velocity shape parameter $\left(\frac{\delta^2}{\nu}\frac{dU}{ds}\right)$.

Subscripts:

T, at transition point.

m, at point of minimum pressure.

RESULTS AND DISCUSSION

Reduction of Data

Velocity calculation.- The method of computing the speed of flow in the N.A.C.A. 8-foot high-speed wind tunnel is described in reference 9. In the computation of the local velocities near the surface of the airfoils, the compressible-flow form of Bernoulli's equation was used. The local air density necessary for the calculations was obtained by assuming adiabatic expansion from the low-speed section of the tunnel where the air temperature is measured. The usual assumption of constant static pressure throughout the depth of the boundary layer was also made.

Constriction effect.- The use of airfoils of large size in comparison with the diameter of the wind tunnel results in an air speed at the airfoil appreciably higher than the speed that would exist if the flow were not restrained by the tunnel walls. The magnitude of this effect was determined by comparing the static pressures measured on the N.A.C.A. 0012 airfoil with results obtained in the full-scale tunnel and with potential-flow theory. For example, at an indicated tunnel air speed of 200 miles per hour, the effective speed at the 5-foot-chord airfoil is 205 miles per hour. The corresponding value for the 2-foot-chord airfoil is 200.8 miles per hour. Throughout this re-

port, the air speed V has been taken as the effective speed obtaining with the airfoil in the tunnel; the dynamic pressure used in reducing the force and the pressure data to coefficient form was based on this effective speed.

Transition

The transition points for the various lift coefficients were determined from curves similar to those shown in figure 4, which may be taken as typical for both the N.A.C.A. 0012 and 23012 airfoil sections. The transition point is defined herein as the point at which the mean velocity near the surface begins to show an abnormal increase owing to the onset of turbulent flow. The region of increasing mean velocity immediately following the transition point is called the transition region.

It will be noticed that the curve for the value of lift coefficient of -0.57 has no well-defined position of minimum velocity and that the behavior of the curve in the region of increasing velocity is very irregular. The transition point for this condition could not be determined except by a study of the shapes of the velocity-distribution profiles, which showed a gradual transition over an extended region.

Upper surfaces of N.A.C.A. 0012 airfoils.- The transition-point locations obtained on the 5-foot-chord metal-covered and solid-wood airfoils are shown together in figure 5 as a function of Reynolds Number for the various test lift coefficients. The slight waviness of the surface of the metal-covered airfoil caused transition to occur somewhat nearer the stagnation point than for the solid-wood airfoil at all test conditions. At the high lift coefficients where transition was controlled mainly by severe adverse pressure gradients, the effect of the waves was small; at $c_l = 0.33$, transition occurred only about 2 percent of the chord nearer the stagnation point than on the ideally fair solid-wood airfoil. As the lift decreased, the effect of the waves became more pronounced and, at a value of c_l of -0.16, caused transition to occur 7 percent of the chord nearer the stagnation point than with the ideal surface conditions. The effect of the waves varied only slightly with change in Reynolds Number.

The transition-point results obtained on the 2- and the 5-foot-chord airfoils of solid construction are shown

together in figure 6. As the surfaces of both of these airfoils were ideally fair and smooth, the results at a given Reynolds Number are strictly comparable. In the range of Reynolds Numbers of 4,000,000 to 7,000,000, transition points were obtained on both sizes of airfoil at widely different speeds and the small differences in transition-point location shown (about 2 percent of the chord on the average) are believed to be due to the effects of the compressibility of the air. The Mach number (ratio of the air speed to the speed of sound in air), upon which compressibility effects depend, varied from 0.29 to 0.59 for the 2-foot-chord airfoil and from 0.11 to 0.20 for the 5-foot-chord airfoil in the overlapping Reynolds Number range of the tests. Compressibility appears to have no pronounced effect on the location of the transition point on a conventional airfoil at low lift coefficients, at least for Mach numbers below 0.60. It should be pointed out that the compressibility shock, which has been found to occur on a body when the maximum local velocity exceeds the local velocity of sound and which is accompanied by radical changes in pressure distribution over the body, had not yet appeared on the N.A.C.A. 0012 airfoil at the maximum speed of the tests.

The static-pressure distribution as obtained by means of the static tube in the boundary-layer survey head is shown in figure 7 for each of the test lift coefficients. The curves represent averages of all the data obtained on the 5-foot-chord airfoils at speeds below 275 miles per hour. The only consistent change in the pressure distribution for speeds greater than 275 miles per hour was a greater negative value of the pressure coefficient P at all stations.

The region in which transition occurred for the N.A.C.A. 0012 airfoils in the present tests is indicated in figure 7 for he four lift coefficients that were tested through the widest range of Reynolds Number. At a given lift coefficient, transition never occurred ahead of the point of minimum pressure and, from the behavior of the curves of figures 5 and 6, the transition point appears to approach the point of minimum pressure, as an approximate forward limit, at Reynolds Numbers of the order of 17,000,000. From a consideration of the probable distance that the laminar flow may extend along the chord at very low Reynolds Numbers, it seems likely that the laminar separation point is a disturbance of sufficient magnitude

to precipitate transition under any conditions. In support of this conjecture, tests on a flat plate (reference 10) showed that transition in an adverse pressure gradient at low Reynolds Numbers occurred at or very near the separation point and resulted in a reattachment of the flow to the surface. The theoretical laminar separation points for the several lift coefficients were estimated by the approximate method of reference 11 and are shown on figure 7. At the lowest Reynolds Numbers, transition occurred in the vicinity, and generally somewhat ahead, of the theoretical separation points. The fact that the transition points for the lift coefficient of 0.33 fell as much as 5 percent of the chord to the rear of the estimated separation points is probably due to the inaccuracy of estimation of separation because no actual separation was observed in the tests at these lift coefficients.

Upper surface of N.A.C.A. 23012 airfoil.- Figure 8(a) shows the variation with Reynolds Number of the transition-point location on the upper surface of the N.A.C.A. 23012 airfoil. It will be noticed that the transition points are given in terms of x/c, chordwise distance from the leading edge. Uncertainty as to the exact stagnation-point location on the N.A.C.A. 23012 airfoil made it inadvisable to employ the parameter s/c used in presenting the N.A.C.A. 0012 airfoil results. The theoretical pressure distribution corresponding to each of the test lift coefficients is given in figure 9(a). The general shapes of the pressure-distribution curves were similar to those for the N.A.C.A. 0012 airfoil, and a direct comparison with the N.A.C.A. 0012 airfoil results can therefore be made. Although the analysis is somewhat handicapped by a scarcity of test points near the extremes of the range of Reynolds Numbers (fig. 8(a)), figure 9(a) shows that transition occurred between the same limits as obtained for the N.A.C.A. 0012 airfoil, namely, the point of minimum pressure and the estimated laminar separation point.

Lower surface of N.A.C.A. 23012 airfoil.- The variation with Reynolds Number of the transition points on the lower surface of the N.A.C.A. 23012 airfoil is shown in figure 8(b) and the corresponding theoretical pressure-distribution curves are shown in figure 9(b). The approximate method of reference 11 for estimating laminar separation could not be satisfactorily applied to this type of pressure distribution. The anomalous behavior of the transition-point curves can, however, be satisfactorily explained, by reference to the results for the N.A.C.A.

0012 airfoil, on the basis of the pressure-distribution diagrams. For all of the lift-coefficient values except 0.30, transition occurred, as on the N.A.C.A. 0012 airfoil, in the adverse pressure gradient back of the point of minimum pressure in spite of the fact that (except at $c_l = 0.65$) there was a subsequent favorable pressure gradient and another peak in each of the pressure-distribution curves. The pressure-distribution curve for $c_l = 0.30$ is intermediate between the type of curve with two well-defined peaks (for $c_l = 0$ and 0.15) and the type with one peak (for $c_l = 0.65$). The curve of transition-point location against Reynolds Number (fig. 8(b)) for $c_l = 0.30$ was also intermediate between the corresponding curves for these two types of pressure distribution.

Comparison with results for a more turbulent air stream.- The difference between the transition-point locations obtained in this investigation on the 5-foot-chord metal-covered airfoil and the faired results obtained in the full-scale tunnel on a 6-foot-chord airfoil of similar construction (reference 5) is shown in figure 10. Since the test conditions and the models employed were made as nearly alike as possible, the difference in the transition points is interpreted to be mainly the result of the difference in air-stream turbulence. Figure 11 shows the differences in pressure distribution on the N.A.C.A. 0012 airfoil as measured in the full-scale and the high-speed tunnels. Because the high-speed-tunnel data shown were measured at low speeds and have been corrected for the effect of constriction, the differences shown are due either to variations in shape and attitude of the models employed or to variations in both. The discrepancies are slight and are believed to have a negligible effect on transition and laminar separation. The greater turbulence present in the full-scale tunnel air stream had a pronounced effect in causing transition to occur nearer the stagnation point than in the present tests. This effect was largest on the pressure side of the airfoil at high lifts and smallest on the suction side at high lifts. The length of the transition region was considerably shorter in the present tests and the transition point was much more sharply defined than in the full-scale-tunnel tests, as is shown in figure 12.

Application of results to free-air conditions.- Although sphere-drag tests in the N.A.C.A. 8-foot high-speed tunnel showed approximately the same critical Reynolds

Number as in flight, it cannot be assumed that the transition results presented in this report will be approximately the same as those obtained on identical airfoils in flight. The small turbulence present in the tunnel had an insignificant effect on transition on a sphere but may have an appreciable influence on airfoil transition. Unpublished results obtained in the model of the N.A.C.A. two-dimensional-flow tunnel, which is believed to have a turbulence level even lower than that of the 8-foot high-speed tunnel, showed the transition points to lie from 2 to 5 percent farther back on the solid-wood airfoil than in the present tests.

Local conditions at the transition point.- The boundary-layer data obtained by means of the four-tube survey-head measurements on the 5-foot-chord N.A.C.A. 0012 metal-covered airfoil permitted an evaluation of parameters describing the local conditions existing near transition. The local Reynolds Number R_s and the boundary-layer Reynolds Number R_δ were computed and are plotted in figures 13 and 14, respectively, as functions of the airfoil Reynolds Number. It is at once apparent that no single values of R_s and R_δ occurred at transition, R_s varying from 570,000 to 3,600,000 and R_δ from about 4,500 to 11,000 with indication of still greater values at larger airfoil Reynolds Numbers. Values of the Reynolds Number R_{δ^*} based on the displacement thickness $U\delta^*/\nu$, which can be obtained experimentally with a higher degree of precision than R_δ, varied from 1,580 to 3,000. A wide range of values of these factors at transition was also reported in reference 5.

The parameters N and λ were computed for comparison with the flight-test results of reference 1. The thickness number N is defined as

$$N = \frac{1}{3} R_{\delta^*}^2 = \frac{1}{3}\left(\frac{U\delta^*}{\nu}\right)^2$$

Pohlhausen's boundary-layer velocity-profile shape parameter λ, having the characteristic value of -12 at the separation point, is defined as

$$\lambda = \frac{\delta^2}{\nu}\frac{dU}{ds}$$

The values of N and λ, shown in figure 15, had

no consistent values at transition. In general, the values of both parameters were numerically less than the values obtained in flight by Jones (reference 1). The values of N lay between 800,000 and 3,000,000 and the values of λ lay between 0 and -6.0. The corresponding flight values (reference 1) for N were 600,000 to 4,800,000 and, for λ, were 0 to -7.2.

There was also computed the nondimensional pressure gradient at transition, which is defined as

$$\frac{s_T}{(1 - P_T)}\left(\frac{dP}{ds}\right)_{\text{at } s_T}$$

where s_T is the value of s at the transition point.

P_T, pressure coefficient at the transition point.

The values of this parameter lay between 0.05 and 0.54 and showed no consistent variation with Reynolds Number.

It thus appears that the fundamental causes of transition cannot be related in a simple way to those local conditions existing at the transition point.

Correlation of transition data on the basis of Reynolds Number and pressure distribution.- An attempt was made to correlate the location of the transition point with the principal controlling factors, Reynolds Number and pressure distribution. An approximate empirical relation between these variables based on the results for the N.A.C.A. 0012 airfoil was obtained. It was assumed that:

1. The laminar layer extends back of the point of minimum pressure a distance depending on the local velocity at this point and the airfoil Reynolds Number.

2. The variation with Reynolds Number of the transition-point location, as experimentally obtained for the zero-lift condition, holds approximately for the other lift coefficients. (See fig. 6.)

For the condition of zero lift on the N.A.C.A. 0012 metal-covered airfoil, the following equation was found

to fit the experimental curve (fig. 6) within the scatter of the test points:

$$\frac{s_T}{c} = 531(R)^{-1/2} + 0.05$$

in which s_T/c is the value of s/c at the transition point. In terms of the location of the point of minimum pressure, s_m/c, and the airfoil Reynolds Number modified for the local velocity at this point, U_m, the expression is

$$\frac{s_T}{c} = \frac{s_m}{c} + 584\left(\frac{RU_m}{V}\right)^{-1/2} - 0.08$$

since, for the zero-lift condition, $\frac{s_m}{c} = 0.13$ and $\frac{U_m}{V} = 1.21$.

In figure 16, the values of this expression are plotted against the measured transition points for all the test conditions of the N.A.C.A. 0012 airfoils and all the upper-surface results of the N.A.C.A. 23012 airfoil. On the same figure are shown the results obtained from the N.A.C.A. full-scale wind-tunnel tests (reference 5), N.A.C.A. flight tests (reference 12), and Jones' flight tests (reference 1). It is seen at once that, for transition points in the range of values of s_T/c from 0 to 0.35, which includes most of the test conditions, the equation can be used to estimate the transition points on the airfoils tested with a probable error of about 3 percent of the chord. For the conditions of very low Reynolds Numbers and the conditions existing on the pressure side of the airfoils at high lifts, for which transition occurs in the range of values of s_T/c from 0.35 to 0.75, the scatter of the points about the mean curve increases but a definite correlation between the measured transition points and the values of this expression exists throughout the entire range. The fact that the flight-test results fall on the same curve as the results from the 8-foot high-speed tunnel is of particular interest, the implication being that the turbulence level in this wind tunnel is low enough to allow approximately free-air transition points to be attained on conventional airfoils. The test results from the full-scale tunnel, however, fall on a well-defined curve considerably dis-

placed from the results from the 8-foot high-speed tunnel and flight, and the indicated effect of turbulence is in general agreement with the indications of figure 10.

Inasmuch as the foregoing method of estimating transition is based on the experimentally determined variation with Reynolds Number of the transition point on the N.A.C.A. 0012 airfoil, it is obviously limited in application to airfoils of conventional section with pressure distributions similar to that of the N.A.C.A. 0012 airfoil, that is, with one peak in the pressure-distribution curve. For example, the relation could logically be applied to the upper and the lower surfaces of the N.A.C.A. 00, 24, 44, and 65 series, to the Clark Y series, and to the Göttingen series of airfoils. It was successfully used to predict transition on the upper surface of the N.A.C.A. 23012 airfoil (see fig. 16), for which the pressure distribution is similar to that for the N.A.C.A. 0012 airfoil. But the pressure distribution on the lower surface of the N.A.C.A. 23012 (see fig. 9(b)) is of a radically different type and the anomalous behavior of the curves of transition-point location against Reynolds Number (see fig. 8(b)) has already been discussed. The expression obviously cannot be employed in this instance.

It is also apparent that the relation is not applicable to conditions where transition is controlled by laminar separation; for example, at very low Reynolds Numbers or on the upper surface at high lifts. In other words, the expression should never be used to predict transition back of the laminar separation point.

Skin Friction

Skin-friction distribution on the N.A.C.A. 0012 airfoil.- The momentum loss per unit span in the boundary layer, M, was obtained from the complete boundary-layer velocity prefiles shown in figure 17 for the condition of zero lift at a Reynolds Number of 10,250,000. On a body such as an airfoil, M may be considered representative of the drag, as a qualitative approximation; and, for a symmetrical airfoil at zero lift, the coefficient $2M/qc$ at any station of measurement therefore represents roughly the contribution to the airfoil drag coefficient of the area ahead of that station.

A plot of the momentum coefficient $2M/qc$ is given

in figure 18 to show the general effect of transition on the drag of the airfoil; the estimated momentum loss, had transition not occurred, is shown as a broken line on the figure. Although the values of M are somewhat lower than the drag, the coefficient dM/dx is nearly equal to dD/dx over the turbulent-flow portion of the airfoil. Thus, at a given station, the difference between the experimental curve, with transition occurring at 20 percent of the chord, and the extended laminar-flow curve should give a close estimate of the increase in drag coefficient resulting from a change in transition point from the station under consideration to the 20-percent-chord station. For example, a movement of the transition point of 10 percent of the chord, from the 30- to the 20-percent-chord station, would result in an increase in the value of the drag coefficient of 0.00111 - 0.00053 or 0.0006. The increases computed in this way are compared later with experimentally determined increments.

The local skin-friction coefficient, plotted in figure 19, was computed from the expression (derived in reference 13, sec. 17, pp. 106-108)

$$c_f = \frac{\tau_o}{q} = \frac{1}{q}\frac{dM}{ds} - \frac{\delta^*}{q}\frac{dp}{ds}$$

where τ_o is the local intensity of skin friction. The sudden increase at transition is followed by a gradual decrease toward the rear of the airfoil owing to the thickening of the turbulent layer and the decrease in the local velocity outside the boundary layer.

Total skin-friction and form drag.- The total skin-friction drag coefficient for the airfoil, c_{d_f}, is equivalent to twice the area under the curve of figure 19 and has the value 0.0047, within limits of accuracy of ± 0.0005. A comparison of this value with the best available estimate of the total profile-drag coefficient of the N.A.C.A. 0012 airfoil $c_{d_o} = 0.0056$ at a Reynolds Number of 10,250,000 (based on an extrapolation of the measurements of reference 14 corrected for transition-point movement) indicates a pressure or form drag between 7 and 25 percent of the total drag.

Estimation of airfoil skin friction.- The measured skin-friction distribution shown in figure 19 makes possible

a comparison of the merits of various methods of estimating airfoil drag when the transition point is known. The relatively small contribution to the total skin friction of the friction of the laminar layer of conventional airfoils at high Reynolds Numbers does not warrant the application of laborious methods such as that of Pohlhausen in computing the laminar skin friction. In the present calculations, the classical flat-plate theoretical values, modified to allow for the increased local velocity due to potential flow, were employed. For a flat plate, the exact local skin-friction coefficient is (reference 13, sec. 14, p. 89)

$$c_f = \frac{0.332}{q}\left(\frac{\mu\rho U^2}{s}\right)^{1/2}$$

where $U = V$. This relation was assumed to hold approximately for an airfoil where $U \neq V$ and was applied in the convenient form:

$$c_f = 0.664\left[\frac{(U/V)^3}{R\ s/c}\right]^{1/2}$$

where U/V is the mean value up to the station s.

The calculated laminar friction is shown in figure 19 and is seen to be a good average approximation for the region of laminar flow. The skin friction computed from the slope of the boundary-layer velocity profiles, which could be obtained with fair accuracy in the laminar-flow region, is also plotted in the figure and indicates satisfactory agreement with the momentum measurements. The relation between the slope and the surface friction is

$$c_f = \frac{\mu}{q}\left(\frac{du}{dy}\right)_{y=o}$$

As a matter of interest, the laminar boundary-layer thickness was computed by the same method of approximation and the agreement between the experimental and the theoretical thickness was good (fig. 20). The approximate equation for the thickness is:

$$\delta = \frac{5.5\ s}{\left(R\ \frac{s}{c}\ \frac{U}{V}\right)^{1/2}}$$

where U/V is the mean value up to the station s.

A method suggested by Dryden and Kuethe in reference 15 was used to compute the skin friction corresponding to the turbulent flow. The principal assumptions were:

(1) The boundary-layer velocity distribution may be described by the relation $u/U = (y/\delta)^{1/7}$ at all stations in the turbulent-flow region.

(2) The skin friction for a given local velocity depends only on the thickness Reynolds Number, according to the results of pipe-flow tests.

Assumption (1) is substituted into the von Kármán integral equation and a solution for δ is obtained; namely,

$$\delta = \left(\frac{0.289\, \nu^{1/4}}{U^{118/28}} \int_0^x U^{27/7}\, dx \right)^{4/5}$$

The velocity-distribution profiles (fig. 17) showed that the end of the transition region was at about 30 percent of the chord; that is, the profiles back of this station showed fully developed turbulent-flow characteristics. Accordingly, δ was computed from the foregoing equation on the assumption that the developed turbulent layer started at a point s_1 (20 percent of the chord) such that the momentum loss at the 30-percent-chord station equaled the measured value at this station. The variation along the chord of the local velocity U was obtained from the experimental results.

By assumption (2), the skin-friction coefficients were then obtained from

$$c_f = 0.045\, \frac{\rho U^2}{2q} \left(\frac{\nu}{U\delta} \right)^{1/4}$$

The results of the calculations of δ and c_f are shown in figures 20 and 19. It is seen that this method gave a fair approximation to the thickness of the turbulent layer (fig. 20) but that the computed skin-friction coefficients (fig. 19) were considerably higher than the measured coefficients.

For small values of δ, the preceding expression is invalid since it gives the result $c_f = \infty$ when $\delta = 0$. The computed turbulent-flow friction curve was therefore extended only to the center of the transition region. If it is assumed that an instantaneous transition takes place at this point ($x/c = 0.25$), the area under the computed curves gives a computed $c_{df} = 0.0053$, which is about 11 percent greater than the measured value.

The foregoing calculations emphasize the fact that, even if the transition point is known, it is impossible to compute airfoil drag with sufficient precision. Adequate data on form drag and on the skin-friction coefficients corresponding to the turbulent flow on airfoils must yet be obtained.

Calculation of scale effect.- The forward movement of the transition point with increasing Reynolds Number (figs. 6 and 8) indicates that the variation with Reynolds Number of the drag coefficient of a smooth airfoil will not follow the skin-friction law for 100-percent turbulent flow as is sometimes assumed for convenience in extrapolating airfoil data. In the calculation that follows, the skin-friction drag coefficient of the N.A.C.A. 0012 airfoil at zero lift is computed for Reynolds Numbers ranging from 1,500,000 to 17,000,000, use being made of the experimentally determined location of the transition point (fig. 6).

The approximate method of computing skin friction previously described is considered adequate for estimating the variation in total skin friction with Reynolds Number although the absolute values of the coefficients will be somewhat high. As before, the boundary-layer flow was considered laminar up to the center of the transition region, which was assumed to lie 5 percent of the chord back of the transition point, i.e., at $s_T/c + 0.05$. Beyond this point, the flow was considered turbulent. An imaginary starting point, s_1, from which the turbulent layer was assumed to develop, was selected for each Reynolds Number so that the momentum loss at the end of transition would have the value $0.00035\ qc$ + laminar drag, determined from the measurements at $R = 10,250,000$. The thickness of the eddying layer was then computed from the Dryden-Kuethe equation, rewritten in terms of the Reynolds Number:

$$\delta_{s/c} = c\left[\frac{0.289}{R^{1/4}}\left(\frac{1}{U/V}\right)^{115/28}\int_{s_1/c}^{s/c}(U/V)^{27/7}\,d(s/c)\right]^{4/5}$$

The airfoil drag coefficient was finally obtained from

$$c_{d_f} = 2.66\left[\left(\frac{U}{V}\right)^3\frac{(s_T/c + 0.05)}{R}\right]^{1/2} + 0.090\left(\frac{c}{R}\right)^{1/4}\int_{(s_T/c\,+0.05)}^{1.00}\left(\frac{U}{V}\right)^{7/4}\delta^{-1/4}\,d(s/c)$$

where the quantity U/V in the term for laminar drag is an average value taken between the leading edge and $s_T/c + 0.05$, and the boundary-layer thickness δ is obtained from the previous equation.

The scale-effect curve thus obtained is shown in figure 21 where it is compared with the special case of 100-percent turbulent flow, that is, where transition occurs at the leading edge. It is seen that the curves have greatly different slopes at the lower Reynolds Numbers and, in addition, are widely separated. The necessity of a detailed consideration of transition effects in estimating the drag of a smooth airfoil is emphasized. The increase in drag due to forward movement of the transition point is more than offset by the decrease of the local skin-friction coefficients with Reynolds Number throughout the range considered. At high Reynolds Numbers, the slopes of the two curves tend to become equal owing to the fact that the motion of the transition point becomes small.

Results of force tests with controlled transition.- The results of the force tests showing the increase in drag associated with controlled movement of the transition point are presented in figure 22. The drag-coefficient increment Δc_d, corresponding to a change in transition-point location $\Delta(x_T/c)$, was defined as follows:

$\Delta c_d = c_d(\text{wing with string}) - c_d(\text{smooth wing}) - c_d(\text{string})$

The drag of the string at a given speed and station was obtained as the difference in drag measured with the string and the carborundum strip because the drag of the carborundum strip, from an estimate based on tests with the wing completely covered with carborundum was negligible. The fact that the straight line through the experimental points does not pass through the origin is probably due to an error in obtaining the basic wing drag, to a possible effect of artificially induced transition by a surface irregularity on the character of transition, or to a combination of these factors. Of paramount interest, however, is the slope of the curve. A comparison of the slope obtained from the momentum-loss diagram (fig. 18) with the slope of the experimental curve shows good agreement. There was practically no change in the slope of the curve, as determined experimentally or as computed, with the original location of transition, with the extent of the transition movement, or with the Reynolds Number. The slope was approximately equal to the estimated profile-drag coefficient so that, as a general rule, for conventional airfoils the drag-coefficient increment in percentage of the profile drag is equal numerically to the change in location of the transition point in percentage of the chord. For example, a small surface irregularity at the 5-percent-chord station on both surfaces of the N.A.C.A. 0012 airfoil would cause transition to occur 37 percent of the chord ahead of the transition-point location on a smooth wing for the condition $c_l = 0$ and $R = 2{,}000{,}000$ (see fig. 6) and would be accompanied by an increase in profile drag of approximately 37 percent. For $R = 10{,}000{,}000$, the increase would be about 20 percent.

CONCLUSIONS

1. The transition point on smooth wings of conventional section in an air stream with turbulence approaching that of free air may be expected to move progressively forward with increasing Reynolds Number from the vicinity of the laminar separation point at Reynolds Numbers of the order 1,000,000 to the vicinity of the point of minimum static pressure at Reynolds Numbers of the order of 17,000,000.

2. Stream turbulence of the magnitude of 0.3 percent had a marked effect in causing transition to occur nearer

the stagnation point, in increasing the length of the transition region, and in reducing the sharpness of definition of the transition point.

3. The effect of compressibility on the location of the transition point on airfoils at low lift coefficients was slight for Mach numbers at least as great as 0.60.

4. Small departures from a fair profile in the form of barely perceptible surface waves may cause transition to occur nearer the stagnation point than on an aerodynamically fair surface.

5. None of the usual parameters describing the local conditions in the boundary layer near transition served as an index for locating transition.

6. For a given stream turbulence, the static-pressure distribution and the Reynolds Number were the main factors influencing the location of the transition point on the airfoils. The transition point on an airfoil of conventional section with a pressure distribution similar to that of the N.A.C.A. 0012 may be expressed as an approximate empirical function of the location of the point of minimum pressure and the Reynolds Number.

7. Present knowledge of form drag and local skin-friction coefficients is inadequate for the precise computation of airfoil drag even though the location of the transition point is known.

Langley Memorial Aeronautical Laboratory,
National Advisory Committee for Aeronautics,
Langley Field, Va., October 21, 1939.

REFERENCES

1. Jones, B. Melvill: Flight Experiments on the Boundary Layer. Jour. Aero. Sci., vol. 5, no. 3, Jan. 1938, pp. 81-101.

2. Dryden, Hugh L.: Air Flow in the Boundary Layer near a Plate. NACA Rep. No. 562, 1936.

3. Dryden, Hugh L., Schubauer, G. B., Mock, W. C., Jr., and Skramstad, H. K.: Measurements of Intensity and Scale of Wind-Tunnel Turbulence and Their Relation to the Critical Reynolds Number of Spheres. NACA Rep. No. 581, 1937.

4. Schubauer, G. B.: The Effect of Turbulence on Transition in the Boundary Layer of an Elliptic Cylinder. Proc. Fifth Int. Cong. Appl. Mech. (Cambridge, Mass.), John Wiley & Sons, Inc., 1939, pp. 321-325.

5. Silverstein, Abe, and Becker, John V.: Determination of Boundary-Layer Transition on Three Symmetrical Airfoils in the N.A.C.A. Full-Scale Wind Tunnel. NACA Rep No. 637, 1939.

6. Robinson, Russell G.: Sphere Tests in the N.A.C.A. 8-Foot High-Speed Tunnel. Jour. Aero. Sci., vol. 4, no. 5, March 1937, pp. 199-201.

7. Platt, Robert C.: Turbulence Factors of N.A.C.A. Wind Tunnels as Determined by Sphere Tests. NACA Rep. No. 558, 1936.

8. Young, A. D., and Maas, J. N.: The Behaviour of a Pitot Tube in a Transverse Total-Pressure Gradient. R. & M. No. 1770, British A.R.C., 1937.

9. Hood, Manley J.: The Effects of Some Common Surface Irregularities on Wing Drag. NACA TN No. 695, 1939.

10. von Doenhoff, Albert E.: A Preliminary Investigation of Boundary-Layer Transition along a Flat Plate with Adverse Pressure Gradient. NACA TN No. 639, 1938.

11. von Doenhoff, Albert E.: A Method of Rapidly Estimating the Position of the Laminar Separation Point. NACA TN No. 671, 1938.

12. Goett, Harry J., and Bicknell, Joseph: Comparison of Profile-Drag and Boundary-Layer Measurements Obtained in Flight and in the Full-Scale Wind Tunnel. NACA TN No. 693, 1939.

13. Prandtl, L.: The Mechanics of Viscous Fluids. Vol. III, div. G of Aerodynamic Theory; W. F. Durand, ed.; Julius Springer (Berlin), 1935.

14. Goett, Harry J., and Bullivant, W. Kenneth: Tests of N.A.C.A. 0009, 0012, and 0018 Airfoils in the Full-Scale Tunnel. NACA Rep. No. 647, 1938.

15. Dryden, H. L., and Kuethe, A. M.: Effect of Turbulence in Wind Tunnel Measurements. NACA Rep. No. 342, 1930.

TABLE I

Distances along the Surface (s/c) from the Theoretical Stagnation Point, Corresponding to Distances along the Chord Line (x/c) from the Leading Edge of the N.A.C.A. 0012 Airfoil

	s/c						
c_l / x/c	-0.57	-0.33	-0.16	0	0.16	0.33	0.65
0	-0.017	-0.010	-0.004	0	0.004	0.010	0.019
.05	.048	.055	.061	.065	.069	.075	.085
.10	.099	.106	.112	.116	.120	.126	.135
.15	.150	.157	.163	.167	.171	.177	.186
.20	.200	.207	.213	.217	.221	.227	.236
.25	.250	.257	.263	.267	.271	.277	.286
.30	.300	.307	.313	.317	.321	.327	.336
.35	.350	.357	.362	.367	.371	.377	.386
.40	.400	.407	.413	.417	.421	.427	.436
.45	.450	.457	.463	.467	.471	.477	.486
.50	.500	.507	.513	.517	.521	.527	.536
.55	.550	.557	.563	.567	.571	.577	.586
.60	.600	.607	.613	.617	.621	.627	.636
.70	.700	.707	.713	.717	.721	.727	.736
.80	.801	.808	.814	.818	.822	.828	.837

L-682

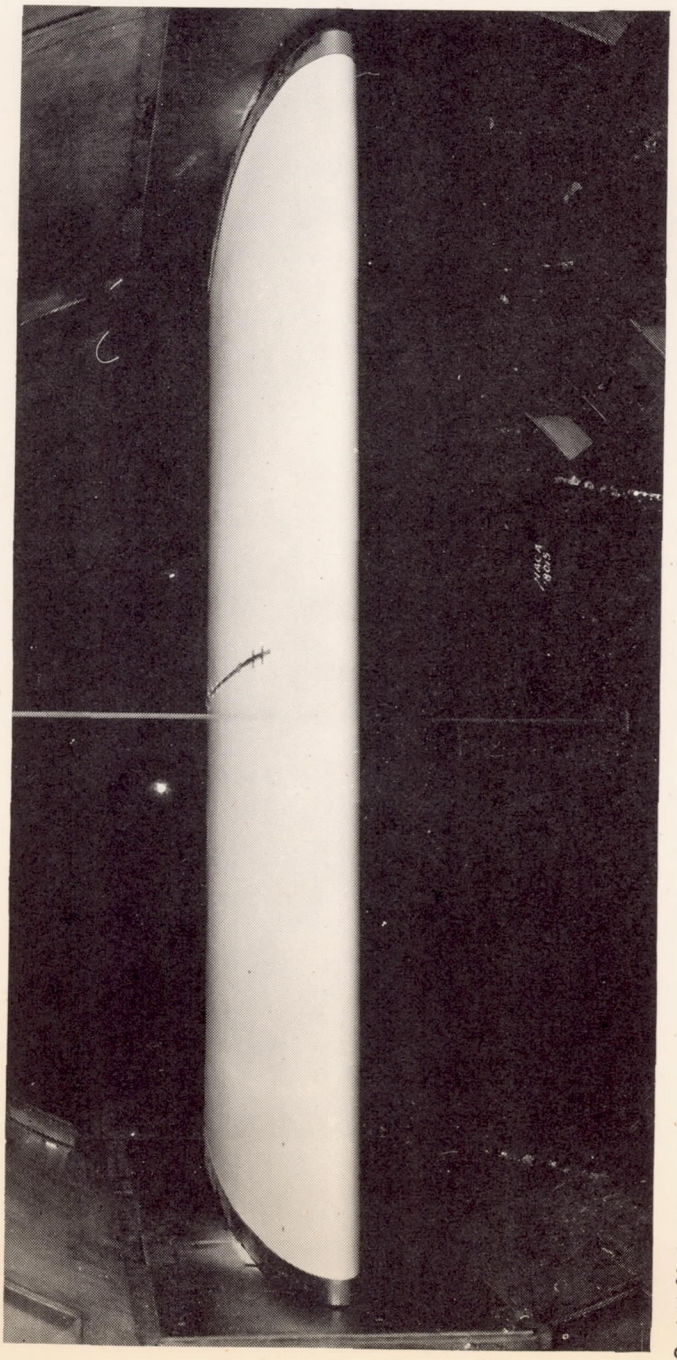

Figure 1.-The 5-foot-chord N.A.C.A. 0012 solid-wood airfoil mounted in the 8-foot high-speed wind tunnel, showing the method of installing the survey tubes.

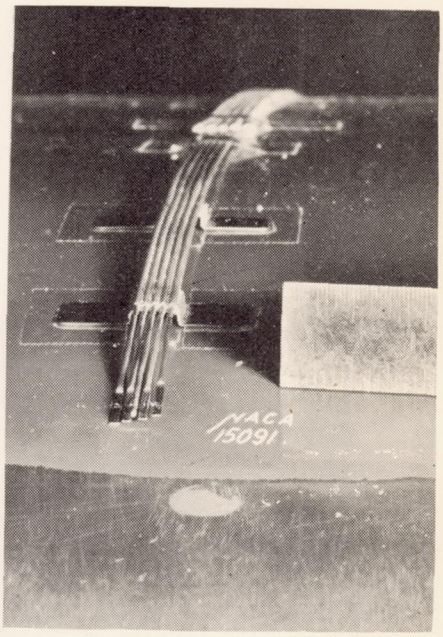

Figure 2.-Static-and total-pressure tubes used in surveying the boundary layer of the 5-foot-chord N.A.C.A. 0012 airfoils.

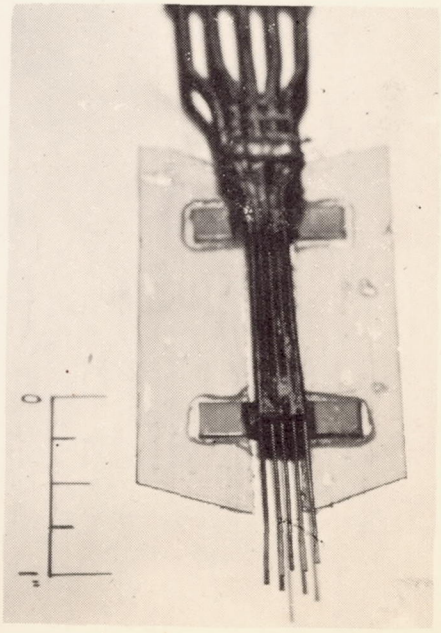

Figure 3.-Static-and total-pressure tubes used in surveying the boundary layer of the 2-foot-chord N.A.C.A. 0012 airfoil. The tubes are approximately two-fifths the size of those used on the 5-foot-chord airfoils.

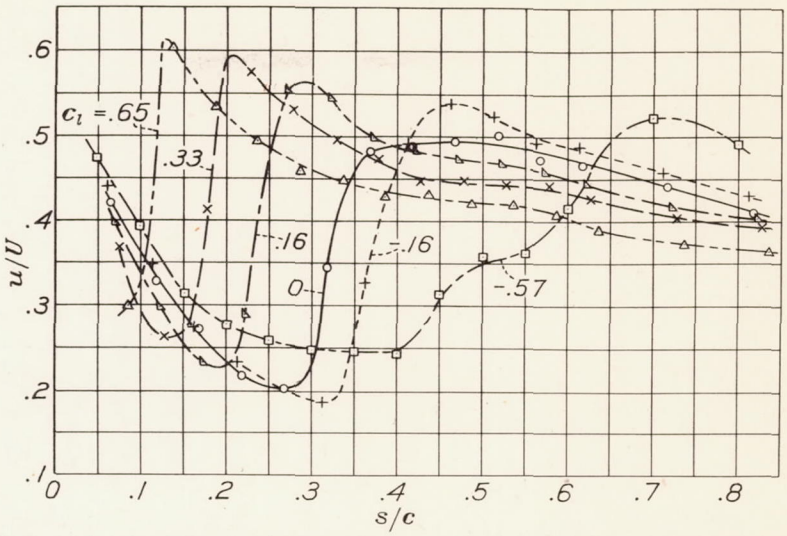

Figure 4.- Velocity in the boundary layer of the 5-foot-chord N.A.C.A. 0012 metal-covered airfoil 0.008 inch above the upper surface at a Reynolds Number of 6,550,000, showing transition at several lift coefficients.

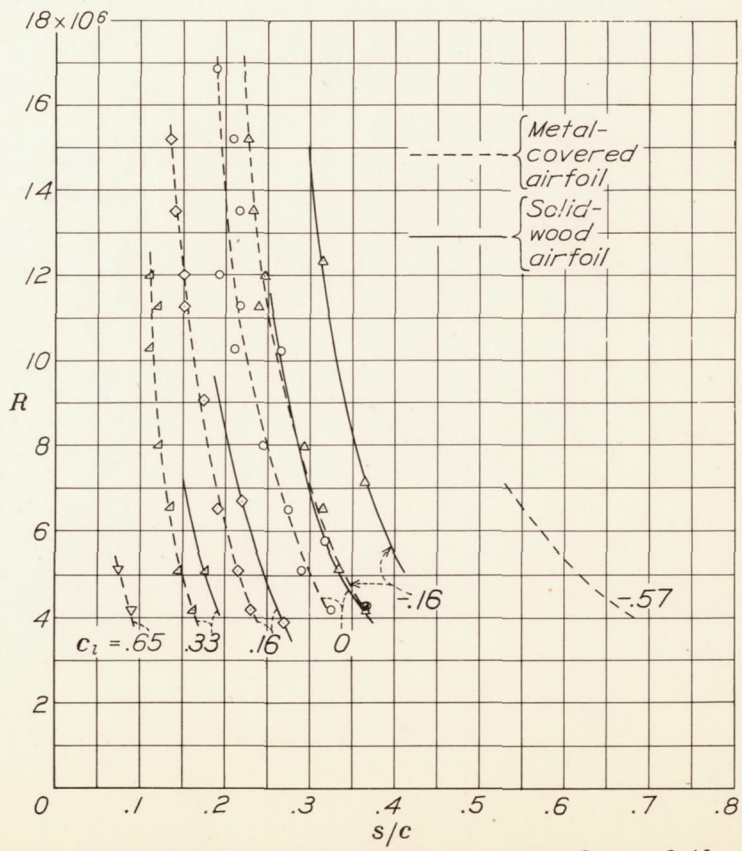

Figure 5.- Transition-point location on the upper surface of the 5-foot-chord N.A.C.A. 0012 airfoils as affected by lift coefficient, Reynolds Number, and minute surface waviness of the metal-covered airfoil.

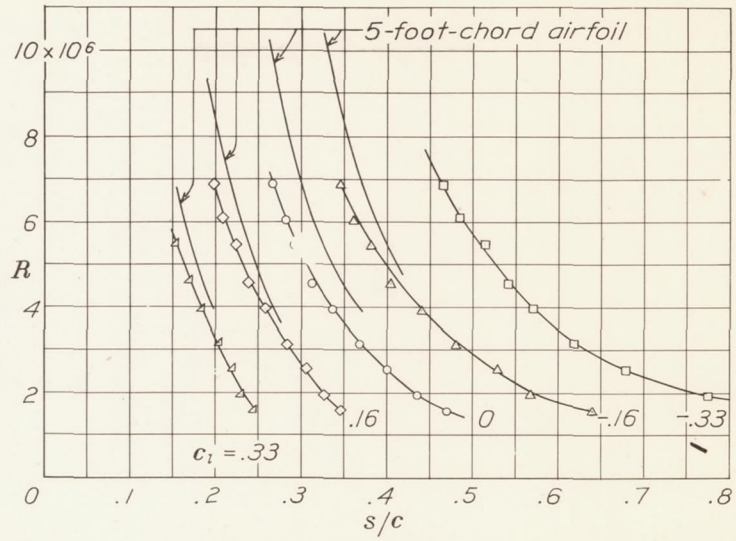

Figure 6.- Transition-point location on the upper surface of the 2-foot-chord N.A.C.A. 0012 airfoil, and comparison with the results for the 5-foot-chord airfoil to show the effect of compressibility.

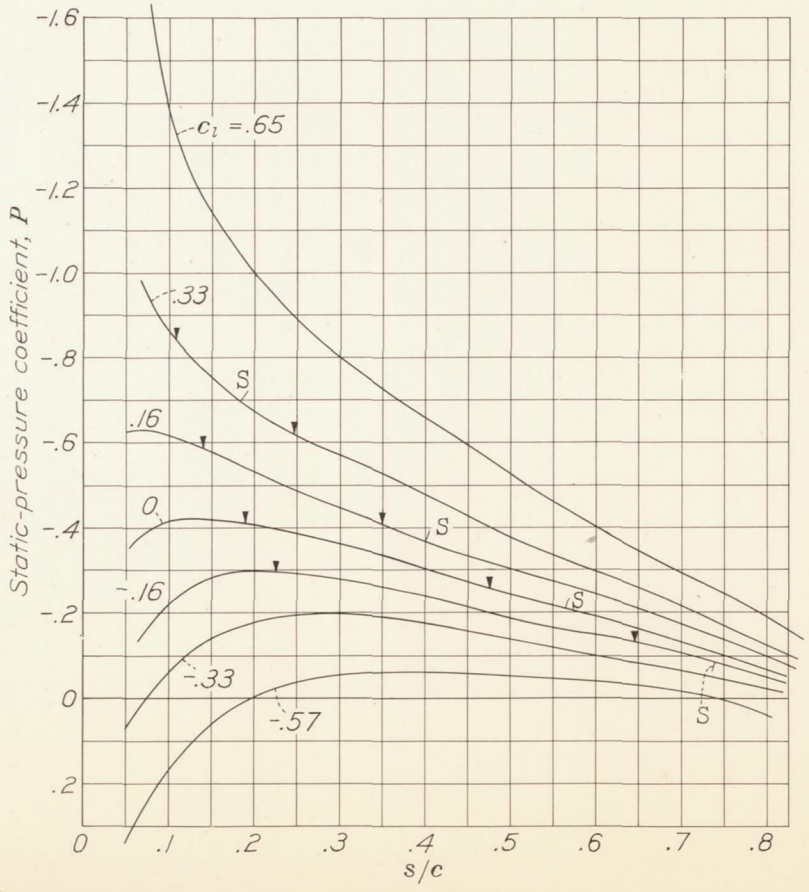

Figure 7.- Static-pressure distribution on the 5-foot-chord N.A.C.A. 0012 airfoil for the test lift coefficients. The ticks indicate the location of the transition points for the extreme test Reynolds Numbers. Estimated laminar separation points are denoted by S.

L-682

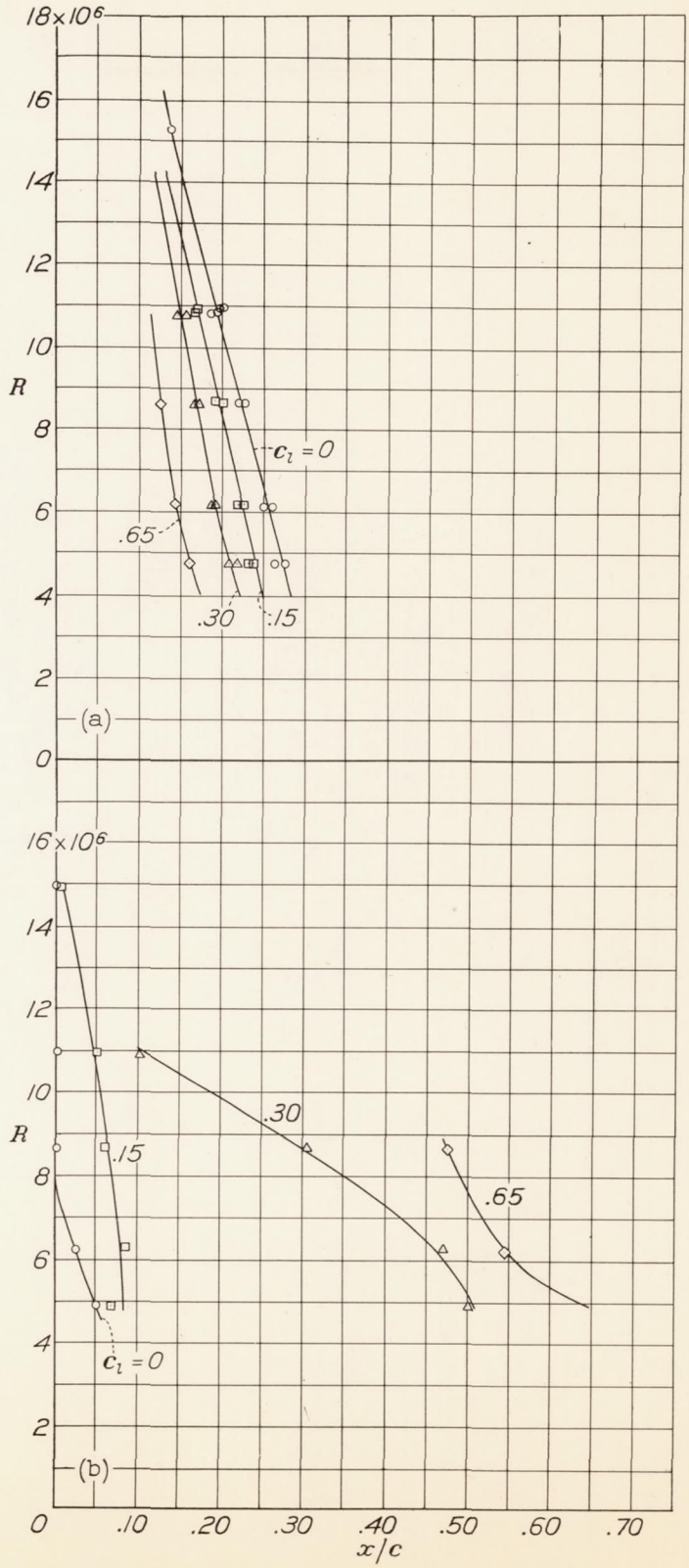

(a) Upper surface. (b) Lower surface.

Figure 8.- Variation with Reynolds Number of the transition point on the N.A.C.A. 23012 airfoil for several lift coefficients.

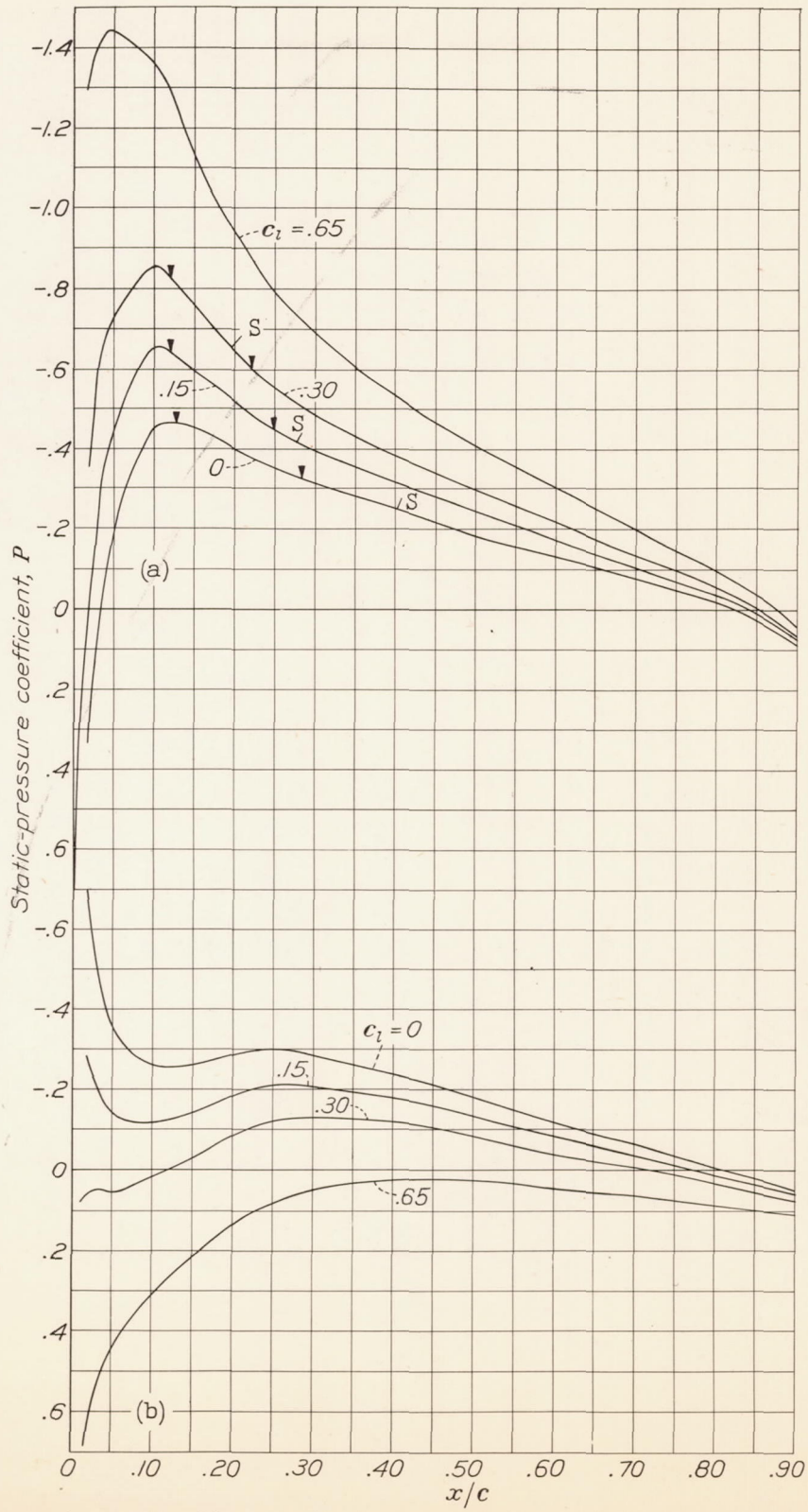

(a) Upper surface. The ticks indicate the location of the transition points for the extreme test Reynolds Numbers. Estimated laminar separation points are denoted by S. (b) Lower surface.

Figure 9.- Theoretical static-pressure distribution on the N.A.C.A. 23012 airfoil for the test lift coefficients.

L-682

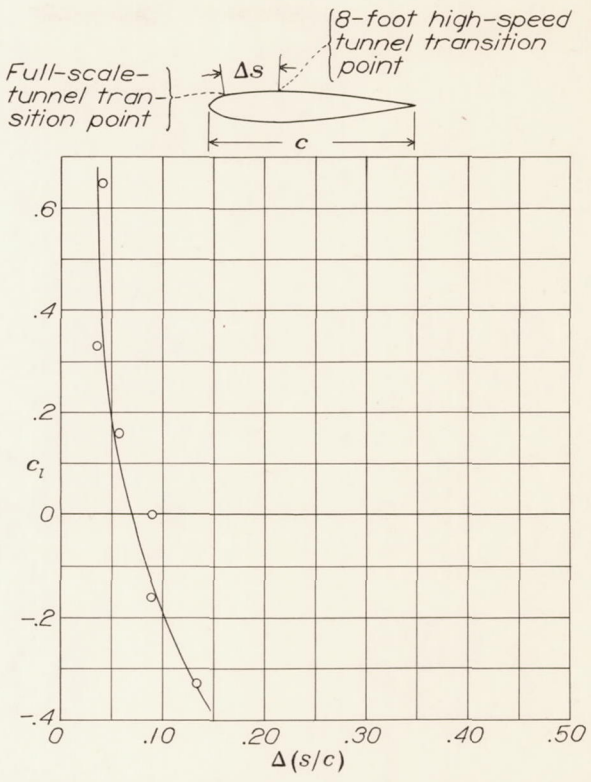

Figure 10.- The difference between the transition-point locations on the upper surface of the N.A.C.A. 0012 metal-covered airfoil as obtained in the 8-foot high-speed and full-scale wind tunnels. R, 5,000,000. (See reference 5.)

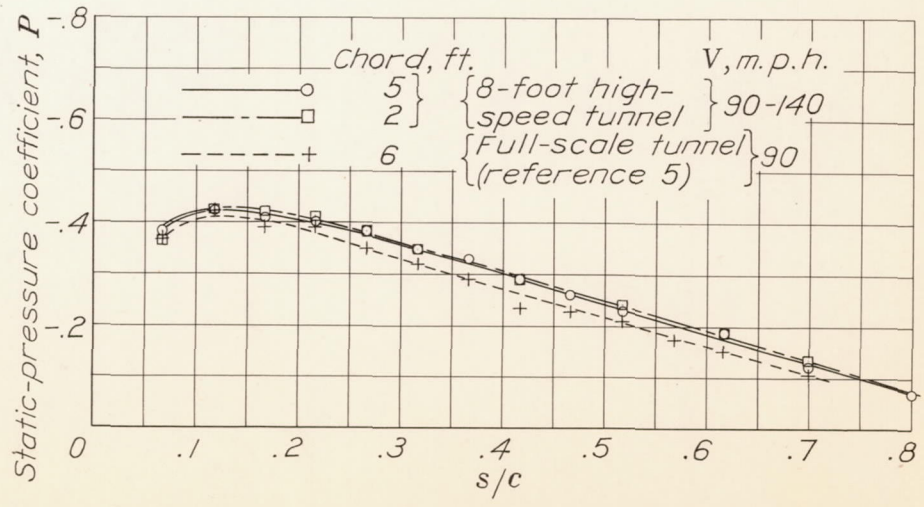

Figure 11.- The static-pressure distribution over the N.A.C.A. 0012 airfoils (corrected for constriction) compared with the results obtained in the full-scale wind tunnel. c_l, 0.

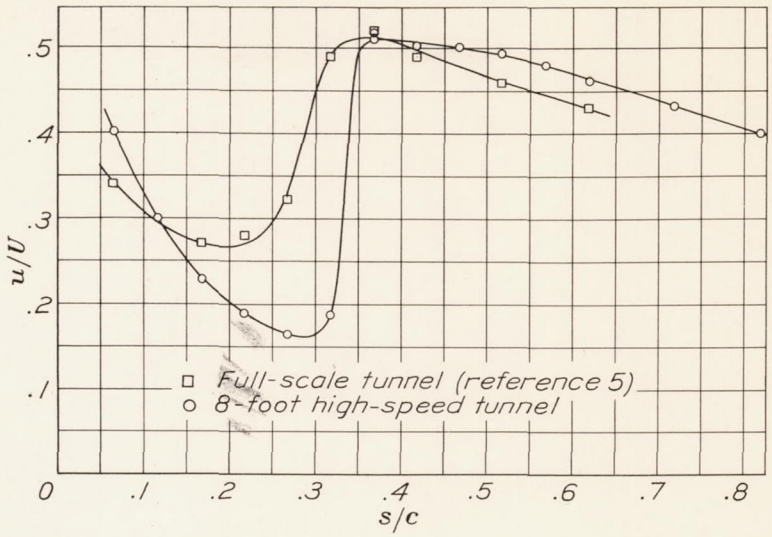

Figure 12.- Comparison of typical transition curves obtained in the 8-foot high-speed and full-scale wind tunnels. c_l, 0; R, approximately 5,000,000.

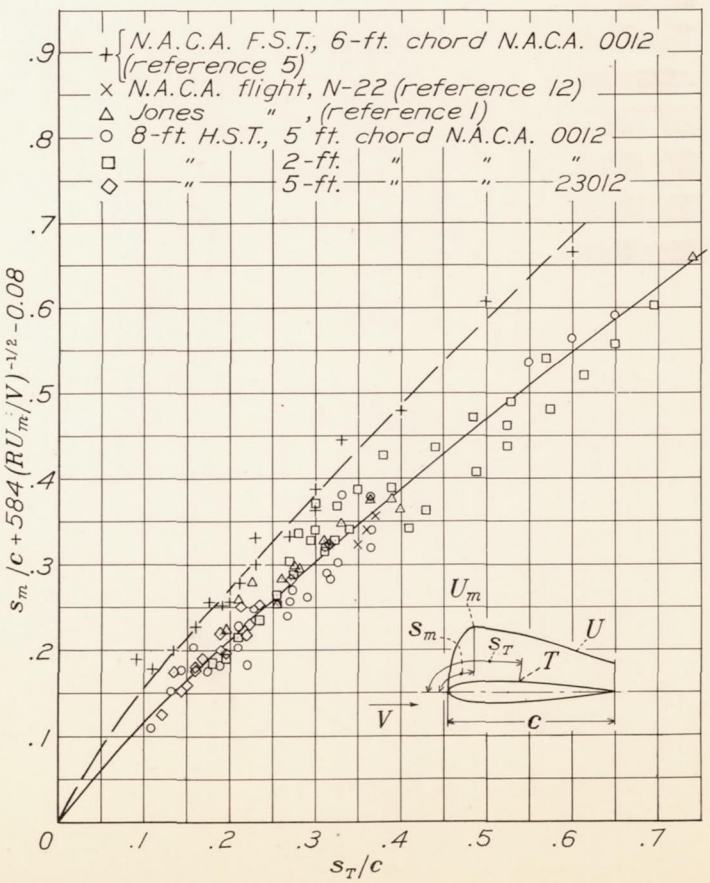

Figure 16.- Correlation of the transition point with pressure distribution and Reynolds Number for the 8-foot high-speed-tunnel test results, and comparison with full-scale-tunnel and flight-test results for several airfoils over a wide range of Reynolds Numbers and lift coefficients.

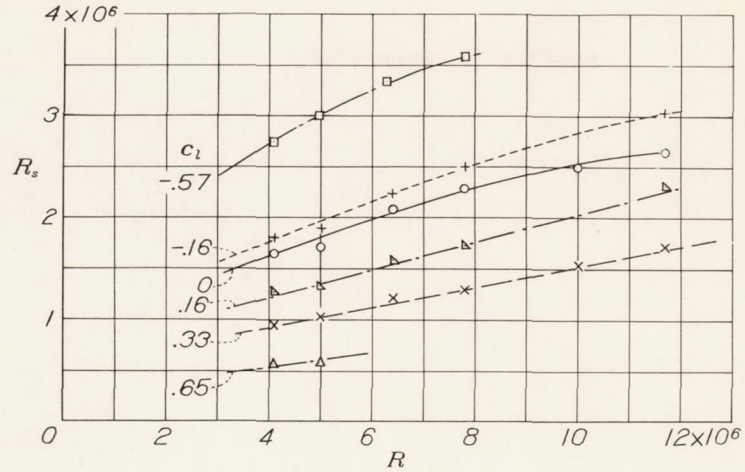

Figure 13.- The local Reynolds Number at the transition point as a function of lift coefficient and Reynolds Number for the 5-foot-chord N.A.C.A. 0012 metal-covered airfoil.

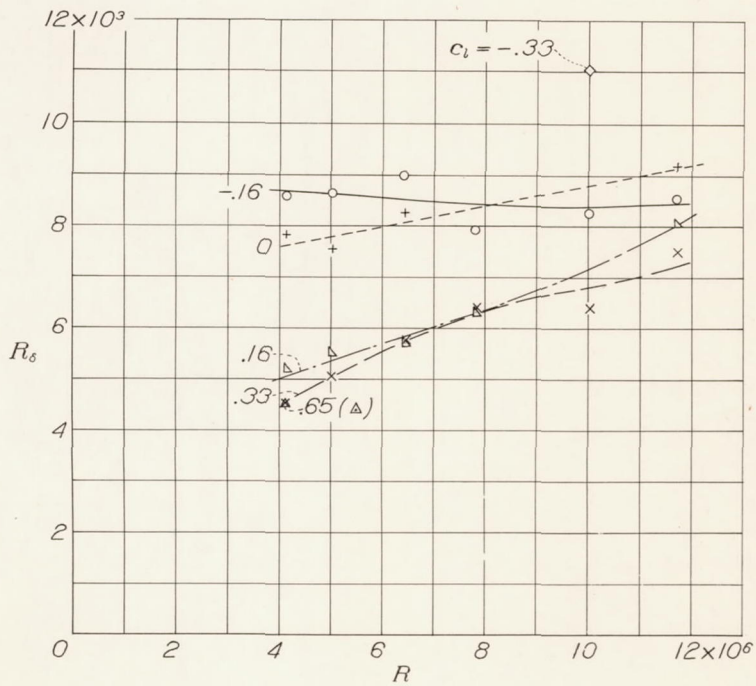

Figure 14.- The boundary-layer Reynolds Number at the transition point as a function of lift coefficient and Reynolds Number for the 5-foot-chord N.A.C.A. 0012 metal-covered airfoil.

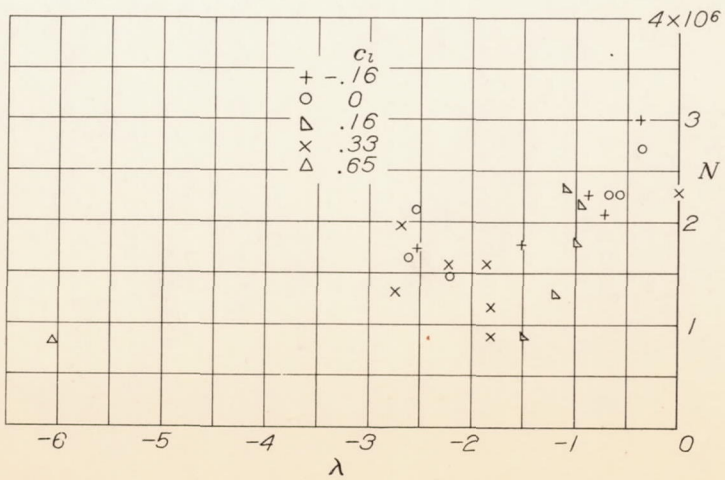

Figure 15.- Values of N and λ at the transition point for the 5-foot-chord N.A.C.A. 0012 metal-covered airfoil.

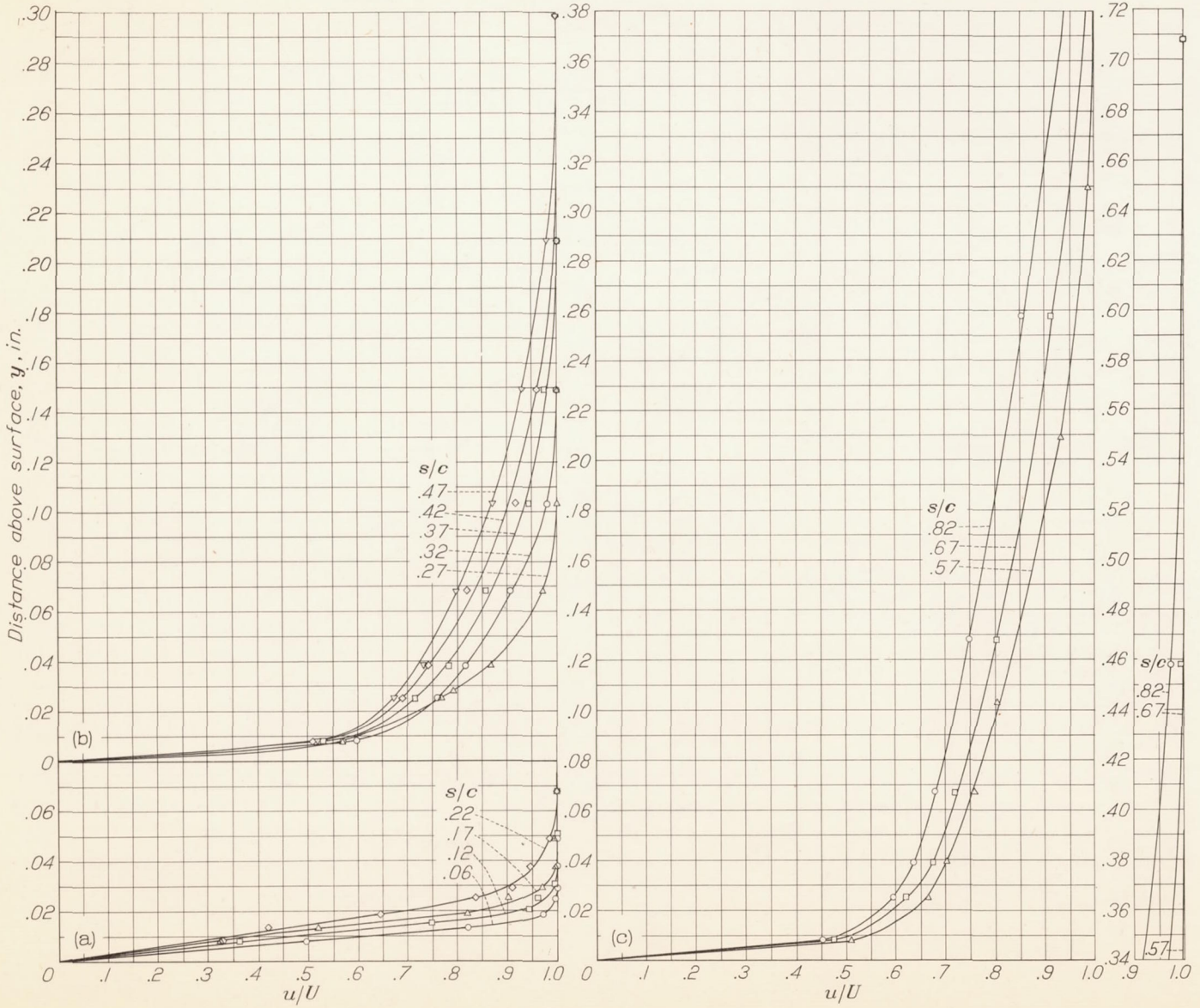

Figure 17.- Velocity profiles in the boundary layer of the N.A.C.A. 0012 airfoil. c_l, 0; R, 10,250,000.

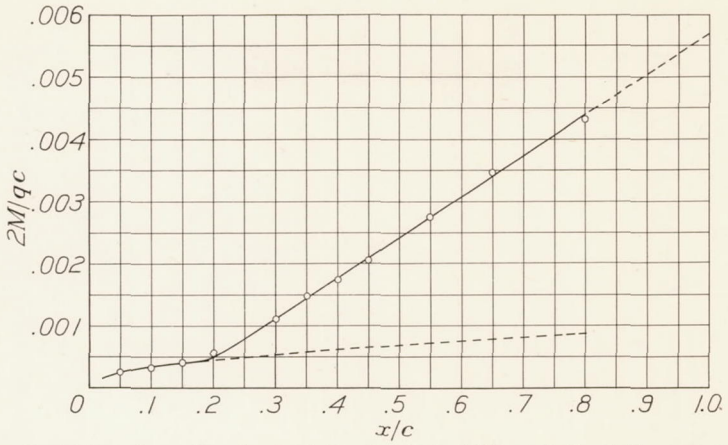

Figure 18.- Variation along the chord of the N.A.C.A. 0012 airfoil of the momentum-loss coefficient. c_l, 0; R, 10,250,000.

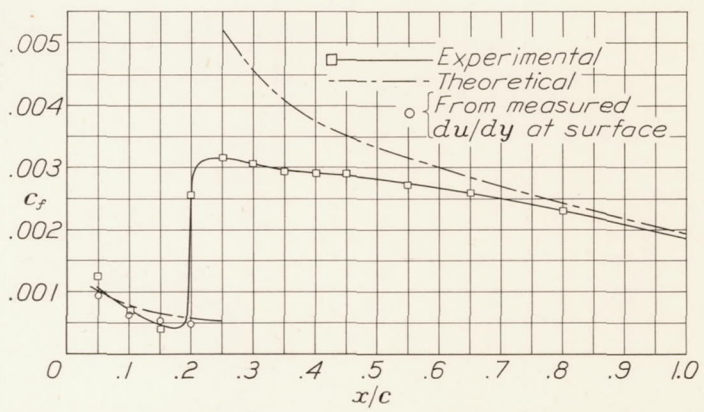

Figure 19.- Variation along the chord of the N.A.C.A. 0012 airfoil of the local skin-friction coefficient and comparison with theoretical approximations. c_l, 0; R, 10,250,000.

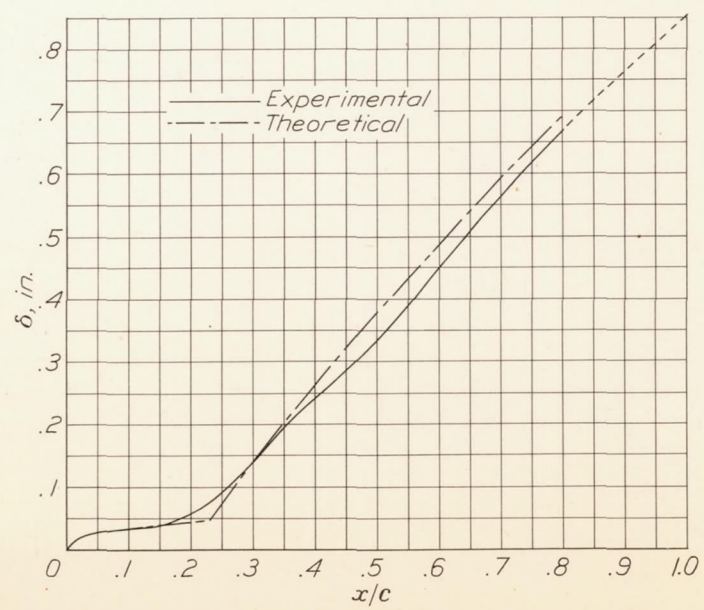

Figure 20.- The thickness of the boundary layer on the N.A.C.A. 0012 airfoil compared with theoretical approximations. c_l, 0; R, 10,250,000.

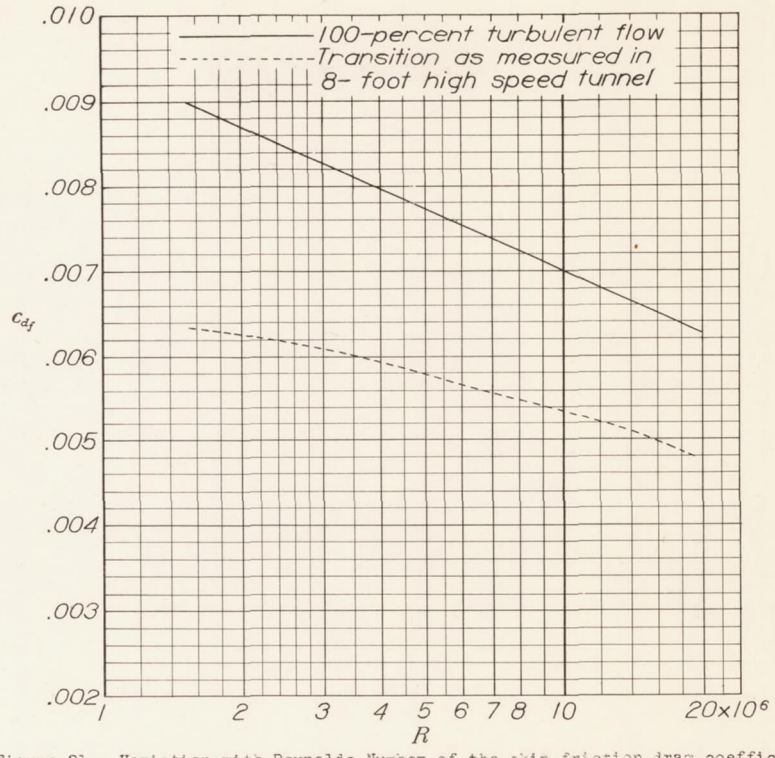

Figure 21.- Variation with Reynolds Number of the skin-friction drag coefficient for the N.A.C.A. 0012 airfoil. (From computations based on the 8-foot high-speed-tunnel transition measurements.) c_l . 0.

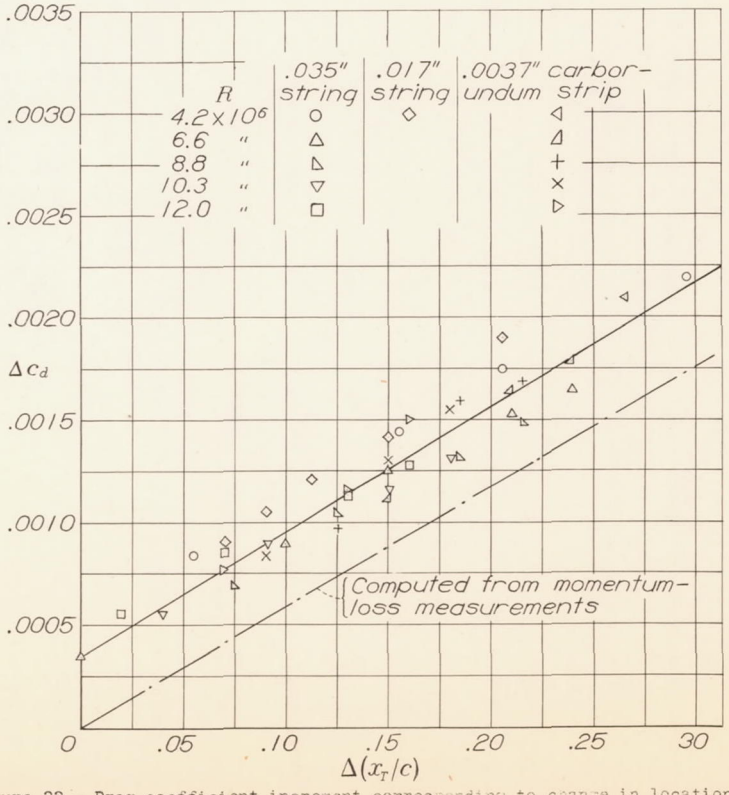

Figure 22.- Drag-coefficient increment corresponding to change in location of the transition point on both surfaces of the N.A.C.A. 0012 airfoil. c_l , 0.